

# High-efficiency synthesis of well-defined cyclic poly(*N*-vinylcaprolactam) and its solution properties



Yaozong Yang, Gang Tang, Minqi Hu, Lidong Shao, Jie Li, Yunmei Bi\*

College of Chemistry and Chemical Engineering, Yunnan Normal University, Kunming 650092, PR China

## ARTICLE INFO

### Article history:

Received 1 April 2015

Received in revised form

2 May 2015

Accepted 13 May 2015

Available online 21 May 2015

### Keywords:

Cyclic poly(*N*-vinylcaprolactam)  
Thermoresponsive phase transition  
behavior  
Supramolecular self-assembly

## ABSTRACT

Well-defined cyclic poly(*N*-vinylcaprolactam) (*c*-PNVCL) was successfully synthesized by a combination of atom transfer radical polymerization (ATRP), supramolecular self-assembly and “selective” click cyclization at a relatively high concentration (10 mg/mL).  $\alpha$ -Alkyne- $\omega$ -chloro heterodifunctional PNVCL precursor (*l*-PNVCL-Cl) was synthesized by ATRP of *N*-vinylcaprolactam (NVCL), followed by its conversion to  $\alpha$ -alkyne- $\omega$ -azido heterodifunctional PNVCL (*l*-PNVCL- $N_3$ ) via nucleophilic substitution reaction with  $\text{NaN}_3$ . The intramolecular cyclization of *l*-PNVCL- $N_3$  by “selective” click reaction in aqueous micellar media afforded well-defined and narrow-disperse *c*-PNVCL (PDI = 1.11). The target polymer and intermediates were characterized by GPC/MALLS,  $^1\text{H}$  NMR, and FT-IR. The thermoresponsive property of *c*-PNVCL and its linear precursor (*l*-PNVCL- $N_3$ ) was studied and compared by turbidity and dynamic light scattering (DLS) measurements, and furthermore, their self-assembly behavior was investigated by fluorescence spectroscopy and transmission electron microscopy (TEM). Cyclic poly(*N*-vinylcaprolactam) can self-assemble to form smaller spherical micelles in aqueous solution and possesses lower critical solution temperature (LCST) and narrower thermal phase transition range in comparison with its linear analogue.

© 2015 Elsevier Ltd. All rights reserved.

## 1. Introduction

Cyclic polymers have attracted much attention for their endless molecular topology, leading to potentially interesting properties for possible further applications [1,2]. They exhibit distinctively unique characteristics and physical properties, such as their compact hydrodynamic volume, lower intrinsic viscosity, and higher thermostability compared to linear analogues [3–8]. In general, the synthesis methods for cyclic polymers include end-to-end ring-closure and ring-expansion polymerization [9–11]. The first method holds the advantage to prepare well-defined cyclic polymers with narrow molecular weight distributions. Although new strategies have been proposed recently [12–16], the combination of controlled/living radical polymerization (CRP) and copper catalyzed azide–alkyne cycloaddition (CuAAC) click reaction has been the most generally used end-to-end polymer cyclization method. To date, this method has been widely used to prepare a series of well-defined cyclic polymers including polystyrene (PS) [11], poly(*N*-isopropylacrylamide) (PNIPAM) [17,18],

poly( $\epsilon$ -caprolactone) [19], poly(acrylic acid) (PAA) [20], poly(methyl methacrylate) (PMMA) [21], poly(methyl acrylate)-*b*-polystyrene [22] and poly(ethylene glycol)-*b*-polycaprolactone [5]. This unimolecular click process has also been employed to construct complex cyclic structures, such as tadpole-shaped and eight-shaped block copolymers [23–25].

Usually, cyclization of linear polymers by coupling end-groups together to form monocyclic polymers need to be conducted by slowly and continuously adding the solution of linear precursors into a highly dilute reaction mixture of solvent and Cu catalyst to suppress the intermolecular reaction. This leads to the production of monocyclic polymer in very low concentrations over long periods of time (>10 h) and at high temperatures (>100 °C). This dramatically reduces efficiency and output for cyclic polymers. Recently, some strategies have been developed to produce cyclic polymers efficiently under more concentrated conditions [26,27]. However, the universality of these strategies still remains largely unexplored.

There are many potential applications of thermoresponsive polymers in drug delivery, tissue engineering, enzyme entrapment, membrane separation and catalysis [28–32]. Poly(*N*-vinylcaprolactam) (PNVCL) is such a thermoresponsive polymer,

\* Corresponding author.

E-mail address: [yunmeibi@hotmail.com](mailto:yunmeibi@hotmail.com) (Y. Bi).

displaying a lower critical solution temperature (LCST) in the physiological range (30–40 °C). Its hydrolysis does not produce small toxic amine compounds as in the case of poly(*N*-isopropylacrylamide) (PNIPAM) which is the most widely studied thermoresponsive polymer. These characteristics, in addition to noncytotoxicity and biocompatibility, suggested that PNVCL is of particular interest for the development in the biomedical field [33–35]. Moreover, the LCST behavior of PNVCL is sensitive to changes of both the polymer chain length and concentration. Thus, the LCST value of PNVCL can easily be modified by controlling the polymer molecular weight with no requirement of using a comonomer [36,37]. Although many linear NVCL-based polymers have been synthesized, little attention has been paid to cyclic PNVCL. Herein, we reported our study on the synthesis of well-defined cyclic PNVCL from  $\alpha$ -alkyne- $\omega$ -azide linear precursor at a relatively high concentration (10 mg/mL) via a combination of supramolecular self-assembly and “selective click” cyclization. To the best of our knowledge, this is the first report of cyclic PNVCL. The thermoresponsive and micellar behaviors of cyclic PNVCL and its linear precursor were also investigated and compared.

## 2. Experimental

### 2.1. Materials

*N*-vinylcaprolactam (98%, Aldrich) was distilled under reduced pressure and then stored at 4 °C. CuCl (97%, Sinopharm Chemical Reagent Co. Ltd., China) was purified by stirring in acetic acid, washed with methanol, and then dried in vacuum. 1,4-Dioxane was distilled over sodium. Dichloromethane (DCM) was distilled from anhydrous calcium chloride for drying. Me<sub>6</sub>Cyclam was synthesized according to the method described in the literature [38]. Triethylamine (TEA, Sinopharm Chemical Reagent, China) was stirred over Na and distilled under reduced pressure. Propargyl alcohol (99%) and CuCl<sub>2</sub> (99.999%) were purchased from Aldrich and used without further purification. 2-Chloropropionyl chloride (99%), sodium azide (NaN<sub>3</sub>, 99%), sodium ascorbate, copper sulfate (CuSO<sub>4</sub>) and other reagents were obtained from Sinopharm Chemical Reagent Co. Ltd. without further purification.

### 2.2. Characterizations

<sup>1</sup>H NMR spectra were determined on a Bruker DRX-500 spectrometer in CDCl<sub>3</sub>. Tetramethylsilicone (TMS) was used as internal standards. Chemical shifts are reported in parts per million (ppm) relative to CDCl<sub>3</sub> (7.26 ppm). FT-IR spectra were taken on a Nicolet AVATAR 360 FT-IR spectrometer. Molecular weight and polydispersity of polymers were measured by gel permeation chromatography/multi-angle laser light scattering (GPC/MALLS). The GPC-MALLS system consisted of a Waters 2690D separations module and a Waters 2414 refractive index detector (RI), and a Wyatt DAWN EOS MALLS detector. Styragel HR1 and HR4 columns (Waters) were used at 40 °C with polystyrene as standards and THF as a mobile phase at a flow rate of 0.3 mL min<sup>-1</sup>. TEM images were obtained using a Hitachi H-600 instrument operating at an acceleration voltage of 80 kV. DLS measurements were performed with a Zetasizer ZEN 3600 instrument (Malvern, UK) operating at 20–50 °C using a light scattering apparatus equipped with a He–Ne laser. The scattering angle was kept at 173° (backscattering) and the wave length in the vacuum was set as 633 nm during the whole experiment. Malvern DTS 6.20 software was used to analyze the data. Each reported measurement was the average of three runs.

### 2.3. Synthesis of propargyl 2-chloropropionate (PCP)

The ATRP initiator, propargyl 2-chloropropionate (PCP) was synthesized by the reaction of propargyl alcohol with 2-chloropropionyl chloride. A mixture of propargyl alcohol (2.0 mL, 33.7 mmol) and TEA (5.6 mL, 37.1 mmol) in dry dichloromethane (DCM) was stirred and cooled to 0 °C in an ice-water bath. 2-chloropropionyl chloride (3.4 mL, 33.8 mmol) in dry DCM was added dropwise to the mixture. The reaction mixture was stirred at 0 °C for another 30 min and then at room temperature for 12 h. The resulting triethylammonium salts were filtrated out, and the filtrate was washed with saturated NaHCO<sub>3</sub> solution and dried over MgSO<sub>4</sub>. After the solvent had evaporated, the remaining product was purified by silica gel column chromatography (petroleum ether–EtOAc, 50: 1) to yielded a yellow oil (4.18 g, yield: 85%). <sup>1</sup>H NMR (CDCl<sub>3</sub>):  $\delta_{\text{H}}$  1.74 (d, J = 2.3 Hz, 3H, CH<sub>3</sub>), 2.55 (s, 1H, C≡CH), 4.46 (m, 1H, CHCl), 4.79 (m, 2H, OCH<sub>2</sub>).

### 2.4. Synthesis of *l*-PNVCL-Cl

*l*-PNVCL-Cl was prepared by ATRP of NVCL. NVCL (610.3 mg, 4.38 mmol), CuCl (3.9 mg, 0.04 mmol), CuCl<sub>2</sub> (0.6 mg, 0.004 mmol), Me<sub>6</sub>Cyclam (12.5 mg, 0.044 mmol), a mixture of 1,4-dioxane and isopropanol were added to a Schlenk flask that was fitted with a rubber septum and pump-filled with nitrogen three times. And then, PCP (6 mg, 0.044 mmol) were added to the flask under nitrogen. The solution was stirred at 30 °C for 2 h. The crude product was dissolved in deionized (DI) water and then transferred to a dialysis bag (MWCO = 3500) and dialyzed against deionized water for 6 days. The final product was dried under vacuum for 24 h, yielding a white solid (overall yield: 58%).

### 2.5. Synthesis of *l*-PNVCL-N<sub>3</sub>

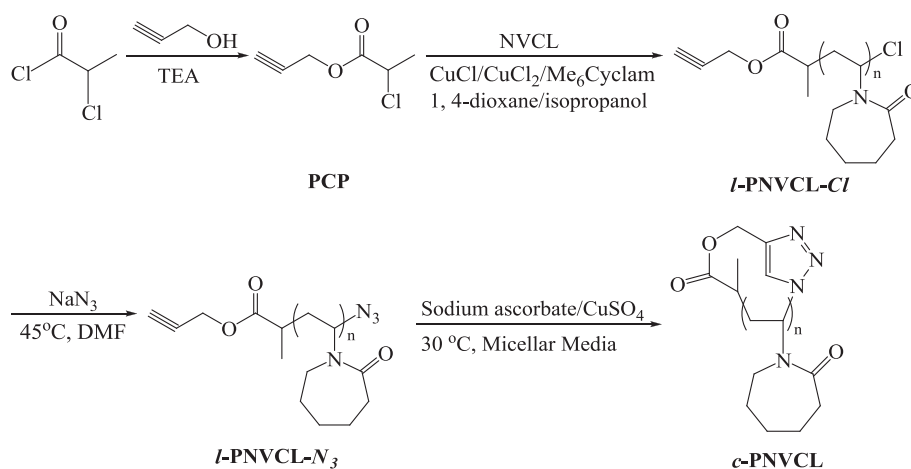
*l*-PNVCL-N<sub>3</sub> was synthesized by the nucleophilic substitution reaction of *l*-PNVCL-Cl with NaN<sub>3</sub>. 8.5 g of *l*-PNVCL-Cl was dissolved in 30 mL of DMF. NaN<sub>3</sub> (325 mg, 5 mmol) was then added and the reaction mixture was stirred at 45 °C for 48 h. After removing DMF under reduced pressure, the remaining product was dissolved in THF and passed through a neutral alumina column to remove residual sodium salts. The resulting product was dried under vacuum for 24 h, yielding a white solid (7.3 g, yield: 93%).

### 2.6. Synthesis of *c*-PNVCL in micellar media

*c*-PNVCL was synthesized via “selective” click reaction in aqueous micellar media. A round bottom flask was charged with *l*-PNVCL-N<sub>3</sub> (400 mg) and water (40 mL). After dissolving at room temperature, the flask was placed in an oil bath thermostated at 30 °C. Sodium ascorbate (50 mg, 0.25 mmol) and CuSO<sub>4</sub> (25 mg, 0.15 mmol) were then added. The reaction mixture was stirred at 30 °C for 24 h before it was removed the solvent and then the remaining product was dissolved in THF and passed through a neutral alumina column to remove residual sodium salts. The product was further purified by precipitation into anhydrous ethyl ether and dried under vacuum for 24 h, yielding a light yellow-colored solid (0.34 g, yield: 85%).

### 2.7. Transmittance measurements

The optical transmittance of aqueous solution of linear or cyclic PNVCL at various temperatures was measured at 500 nm with a UV-vis spectrometer (CARY UV-50, VARIAN) equipped with a water-circulation heating stage. The heating rate was 1 °C/5 min.



**Scheme 1.** Synthesis of cyclic poly(*N*-vinylcaprolactam) (*c*-PNVCL).

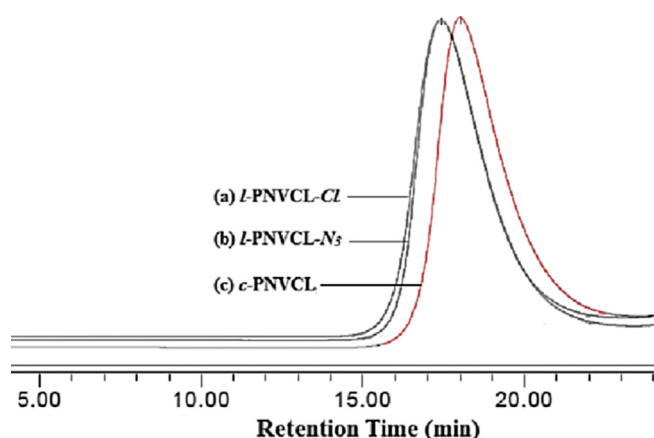


**Fig. 1.** GPC traces of *l*-PNVCL-Cl (a), *l*-PNVCL- $N_3$  (b), and *c*-PNVCL (c).

The lower critical solution temperature (LCST) was defined as the temperatures corresponding to 1% decreases of transmittance [17].

### 2.8. Preparation of PNVCL micelles

The micelles were prepared from *l*-PNVCL- $N_3$  and *c*-PNVCL according to the literature [39]. In a typical procedure, distilled water (10 mL) was added dropwise to a THF solution of *l*-PNVCL- $N_3$  (10 mg/mL, 2 mL). The solution was dialyzed against distilled water for 24 h and then vacuum dried for 72 h. Dried micelles (10 mg) was dispersed in distilled water (10 mL). The micellar solution was kept for a week at room temperature, and then was filtered through a 0.45  $\mu\text{m}$ -pore membrane filter before it was characterized by TEM and DLS.

### 2.9. Fluorescence measurements

The critical micellization concentrations (CMC) of *l*-PNVCL- $N_3$  and *c*-PNVCL were determined by the fluorescence technique using pyrene as a probe. Aliquots of pyrene solution ( $5 \times 10^{-5}$  M in acetone, 5  $\mu\text{L}$ ) were added to volumetric flasks, and the acetone was evaporated. The aqueous solutions of *l*-PNVCL- $N_3$  or *c*-PNVCL at different concentrations were added to the flasks to get a final pyrene concentration of  $4 \times 10^{-7}$  M. The mixture solutions were sonicated for 30 min and then kept at room temperature for 24 h before measurements. Fluorescence spectra were recorded on a Hitachi F-4500 luminescence spectrophotometer with a band width of 5 nm for excitation and emission. Excitation was carried out at 334 nm, and emission spectra were recorded ranging from 350 nm to 550 nm.

## 3. Results and discussion

The synthetic procedure of cyclic poly(*N*-vinylcaprolactam) (*c*-PNVCL) was presented in Scheme 1. It involves preparation of well-defined  $\alpha$ -alkyne- $\omega$ -chloro heterodifunctional PNVCL (*l*-PNVCL-Cl) by ATRP of NVCL, followed by reacting with  $\text{NaN}_3$  to transform the terminal chloride into azide group, and the subsequent intramolecular cyclization by “selective” click reaction in aqueous micellar media at a relatively high concentration (10 mg/mL).

### 3.1. Synthesis and characterization of linear PNVCL precursors

It is well known that ATRP of *N*-vinylcaprolactam (NVCL) is not an easy task plausibly owing to deactivation of the copper catalyst through complexation with amide groups, the substitution of halide from the propagating chain ends by amide, and the low values of the ATRP equilibrium constant. Recently, situation has

**Table 1**  
Characterizations of linear PNVCL precursors and cyclic PNVCL.

Polymers	$M_{n, \text{theo}}^a$ (g/mol)	$M_{n, \text{NMR}}^b$ (g/mol)	$M_{n, \text{GPC}}^b$ (g/mol)	PDI <sup>b</sup>	$M_p^b$	G factor <sup>c</sup>	CMT <sup>d</sup> (°C)
<i>l</i> -PNVCL-Cl	6116	6263	21,900	1.14	41,400	—	—
<i>l</i> -PNVCL- $N_3$	—	—	22,000	1.13	41,500	—	28
<i>c</i> -PNVCL	—	—	17,100	1.11	33,200	0.80	26

<sup>a</sup> The theoretic molecular weight was calculated by the formula:  $M_{n, \text{theo}} = M_{\text{monomer}} \times [\text{monomer}]/[\text{initiator}] \times \text{Conversion\%} + M_{\text{initiator}}$ .

<sup>b</sup>  $M_n$ ,  $M_p$  and PDI were determined by GPC/MALLS.

<sup>c</sup> The ratio of the apparent peak molar masses ( $M_{pc}/M_{pl}$ ) corresponding to *c*-PNVCL and *l*-PNVCL- $N_3$ .

<sup>d</sup> Critical micellization temperatures (CMT) determined by temperature-dependent optical transmittance changes in aqueous solution at a concentration of 10 mg/mL.

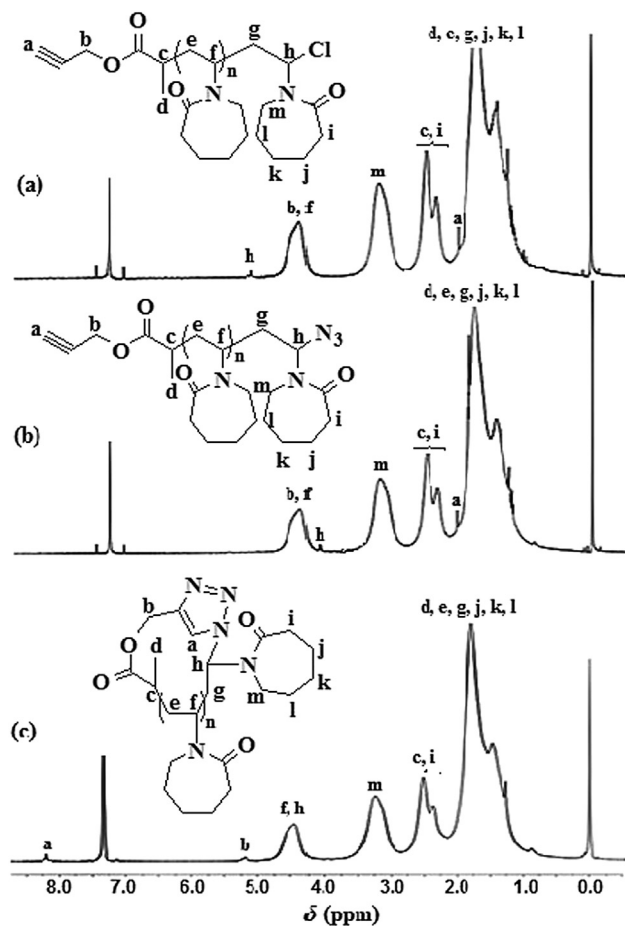


Fig. 2.  $^1\text{H}$  NMR spectra of *l*-PNVCL-Cl (a), *l*-PNVCL- $\text{N}_3$  (b), and *c*-PNVCL (c).

been improved. Singh et al. reported the ATRP of NVCL by using the powerful ATRP catalyst CuBr/PMDETA and ethyl-2-bromoisobutyrate (EIB) as initiator in 1,4-dioxane, resulting in PNVCL with polydispersity indices (PDI) between 1.21 and 1.40 [40]. Jiang et al. prepared poly(tert-butyl acrylate)-*g*-poly(*N*-vinylcaprolactam) (PtBA-*g*-PNVCL, PDI  $\leq 1.32$ ) by ATRP of NVCL using CuBr/Me<sub>6</sub>Cyclam as the catalytic system and Br-containing PtBBPMA backbone as initiator in 1,4-dioxane [41]. Our group successfully synthesized poly(DL-lactide)-*b*-poly(*N*-vinylcaprolactam) (PDLLA-*b*-PNVCL) block copolymers with low molecular weight distributions (PDI  $\leq 1.26$ ) by ATRP of NVCL using PDLLA-Cl/CuCl/CuCl<sub>2</sub>/Me<sub>6</sub>Cyclam system in 1,4-dioxane [39]. In this study, a similar protocol was employed for the ATRP of NVCL monomer.  $\alpha$ -Propargyl- $\omega$ -chloro heterodifunctional PNVCL, *l*-PNVCL-Cl was synthesized by ATRP of NVCL using propargyl 2-chloropropionate (PCP) as initiator, Me<sub>6</sub>Cyclam as ligand, CuCl/CuCl<sub>2</sub> as catalysts at 30 °C in the mixture solvent of 1,4-dioxane and isopropanol. The addition of small amounts of deactivating CuCl<sub>2</sub> is capable of improving the control of molecular weights and polydispersity [42]. The mixture solvent of 1,4-dioxane and isopropanol can dissolve monomer, polymer and catalyst, permitting optimization of the polymerization. The hydrogen bonding between the isopropanol and cyclic amide groups of NVCL may alleviate, but not eliminate, catalyst deactivation [43]. The nucleophilic substitution reaction of the chlorine group at the end of *l*-PNVCL-Cl with NaN<sub>3</sub> yielded the desired linear PNVCL precursor, *l*-PNVCL- $\text{N}_3$ .

The linear PNVCL precursors were characterized by GPC/MALLS,  $^1\text{H}$  NMR, and FT-IR. *l*-PNVCL-Cl precursor shows unimodal and

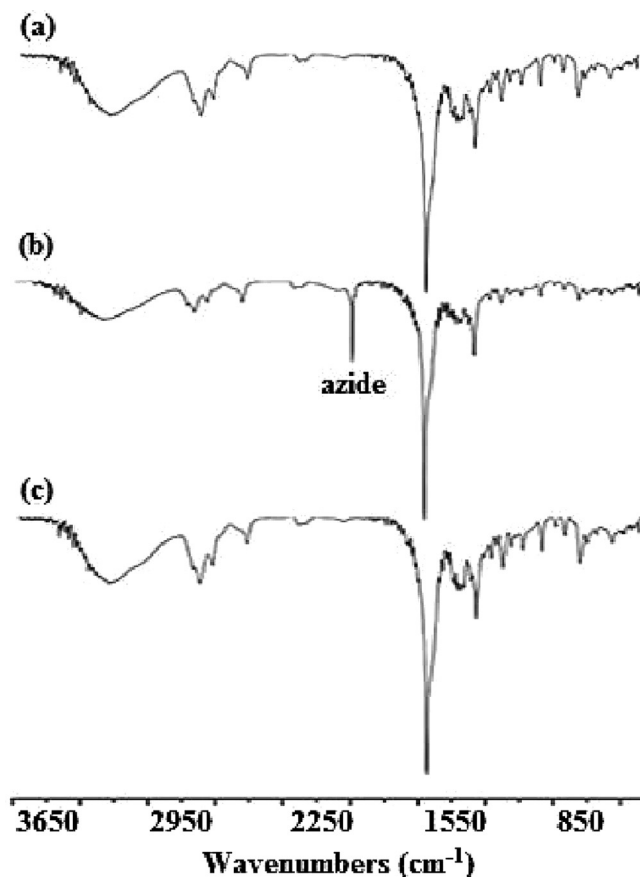


Fig. 3. FT-IR spectra of *l*-PNVCL-Cl (a), *l*-PNVCL- $\text{N}_3$  (b), and *c*-PNVCL (c).

symmetric GPC trace (Fig. 1a) with low polydispersity indices (PDI = 1.14) (Table 1), which reveals that no detectable tail or shoulder peak at lower or higher MW position attributed to premature chain termination polymer was observed. In the  $^1\text{H}$  NMR spectrum of *l*-PNVCL-Cl (Fig. 2a), the peak at 5.46 ppm corresponds to methine proton adjacent to the terminal chlorine. The  $M_{n,\text{NMR}}$  value of *l*-PNVCL-Cl was determined by comparing the peak integration ratio of the PNVCL protons at 3.22 ppm for NCH<sub>2</sub> group to methine proton adjacent to the terminal chlorine at 5.46 ppm. The  $M_{n,\text{NMR}}$  value of *l*-PNVCL-Cl was consistent with its  $M_{n,\text{theo}}$  value (Table 1), confirmed that well-defined *l*-PNVCL-Cl precursor was successfully synthesized by ATRP of NVCL. The difference between  $M_{n,\text{GPC}}$  value of *l*-PNVCL-Cl and its  $M_{n,\text{theo}}$  value may be owing to the different structure between PNVCL and polystyrene standard. GPC trace in Fig. 1b show that the elution peak of *l*-PNVCL- $\text{N}_3$  is almost the same as that of *l*-PNVCL-Cl. In the  $^1\text{H}$  NMR spectrum of *l*-PNVCL- $\text{N}_3$  (Fig. 2b), a new peak appears at 4.15 ppm, corresponding to the methylene protons adjacent to the terminal azide group, whereas the peak at 5.46 ppm disappears. Compared to the FT-IR spectrum of *l*-PNVCL-Cl (Fig. 3a), a new peak at 2108  $\text{cm}^{-1}$  belonged to the characteristic absorption of the terminal azido group is observed in FT-IR spectrum of *l*-PNVCL- $\text{N}_3$  (Fig. 3b). All the above data provide strong evidence for near-quantitative formation of azide end-groups.

### 3.2. Synthesis and characterization of well-defined cyclic poly(*N*-vinylcaprolactam)

It has been reported that water-soluble cyclic diblock copolymers can be prepared via the combination of supramolecular

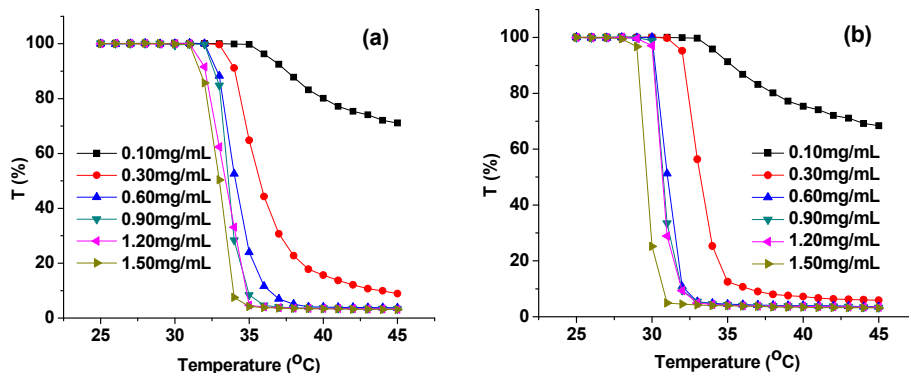


Fig. 4. Transmittance measurements as a function of temperature for different concentrations of *l*-PNVCL-*N*<sub>3</sub> (a) and *c*-PNVCL (b).

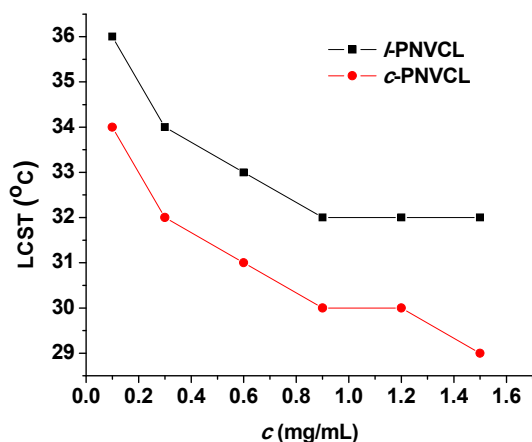


Fig. 5. Concentration dependences of LCST obtained for aqueous solutions of *l*-PNVCL-*N*<sub>3</sub> and *c*-PNVCL.

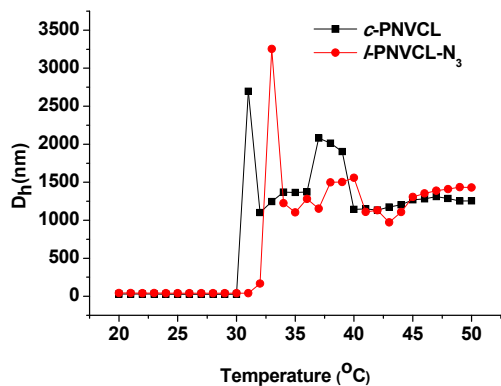


Fig. 6. Plots of hydrodynamic diameters (*D*<sub>h</sub>) of the formed micelles by *l*-PNVCL-*N*<sub>3</sub> and *c*-PNVCL in aqueous solution as a function of temperature from DLS measurements.

self-assembly and “selective” click reaction, which takes advantage of the unimer-micelle exchange equilibrium [26]. It is quite expected that this strategy can be employed for the synthesis of cyclic poly(*N*-vinylcaprolactam) (*c*-PNVCL) since *l*-PNVCL-*N*<sub>3</sub> molecularly dissolves in aqueous solution at room temperature and is able to self-assemble into micelles consisting of carbon–carbon backbone chain cores and well-solvated cyclic amide groups coronas in aqueous solution at elevated temperatures (Table 1). The terminal

alkynyl group may be close to carbon–carbon backbone or cyclic amide while azide group may be adjacent to cyclic amide or carbon–carbon backbone. Within self-assembled aggregates, the terminal alkynyl group or azide group close to carbon–carbon backbone was buried inside the hydrophobic core of the micelles while azide or alkynyl group adjacent to cyclic amide is located at the corona surface. In the two cases, reactive terminal alkynyl and azide moieties are spatially separated which result in the click reactions within micelles will not occur. But intramolecular click cyclization can occur exclusively for unimers because of its low concentration (CMC) [26]. This permits the facile preparation of cyclic poly(*N*-vinylcaprolactam) (*c*-PNVCL) from *l*-PNVCL-*N*<sub>3</sub> at relatively high concentration. Thus, the intramolecular “click” cyclization of *l*-PNVCL-*N*<sub>3</sub> (400 mg in 40 mL of water) was carried out in aqueous micellar media at 30 °C for 24 h in the presence of CuSO<sub>4</sub> and sodium ascorbate. The successful intramolecular cyclization reaction was confirmed through analyzing the linear precursor and cyclization product by FTIR, <sup>1</sup>H NMR and GPC. Fig. 3c shows that the characteristic azide absorbance peak at 2108 cm<sup>-1</sup> completely disappeared after the click reaction. In the <sup>1</sup>H NMR spectrum of the cyclization product (*c*-PNVCL) (Fig. 2c), compared to the linear precursor, the peak at 2.06 ppm corresponding to the alkyne proton and the peak at 4.15 ppm disappear, while new peaks come out at 8.19 and 5.17 ppm, corresponding to the proton of triazole ring and methylene protons immediately adjacent to the triazole, respectively. The characteristic increase in the GPC retention time of the *c*-PNVCL (Fig. 1c), in comparison with its linear precursor (*l*-PNVCL-*N*<sub>3</sub>), was used to verify cyclization, as the cyclic polymer has a more compact structure with a smaller hydrodynamic volume and therefore a slower elution. Additionally, *c*-PNVCL remained monomodal in nature and retained its low polydispersity (Table 1), indicated that intermolecular reaction products were not produced as a byproduct during the cyclization process. The G factor, the ratio of the apparent peak molar masses (*M*<sub>pc</sub>/*M*<sub>pl</sub>) corresponding to cyclic and linear polymer derived from GPC traces can reflect the cyclization efficiency. The G value of PNVCL was 0.80 (Table 1), a value comparable to those reported for other cyclic vinyl polymers (0.70–0.97) [44–46].

### 3.3. Thermal phase transition behavior of *l*-PNVCL-*N*<sub>3</sub> and *c*-PNVCL

The thermal phase transitions of *l*-PNVCL-*N*<sub>3</sub> and *c*-PNVCL were investigated with temperature-dependent turbidity. In order to compare with thermoresponsive phase behavior of linear-PNIPAM-*N*<sub>3</sub> and cyclic-PNIPAM [17] conveniently and directly, in this study, LCST value was defined as the temperature at which 1% decreases of transmittance could be observed. Fig. 4 shows the transmittance of the polymers as a function of temperature with

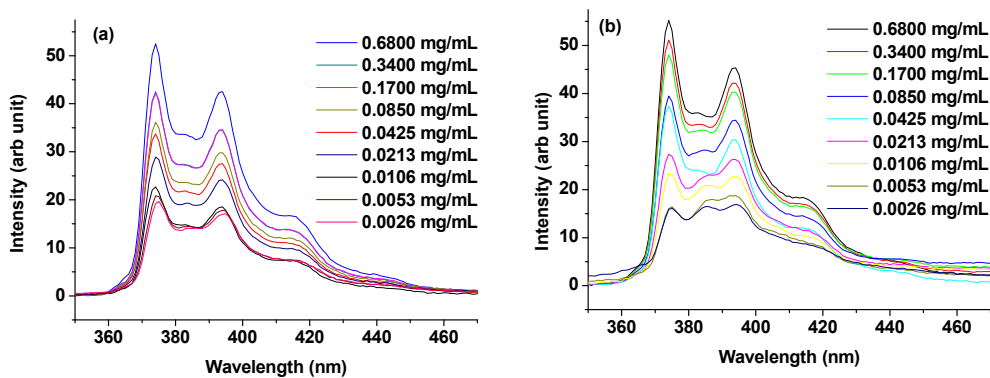


Fig. 7. Fluorescence spectra of pyrene in water at different concentrations of *l*-PNVCL-*N*<sub>3</sub> (a) and *c*-PNVCL (b).

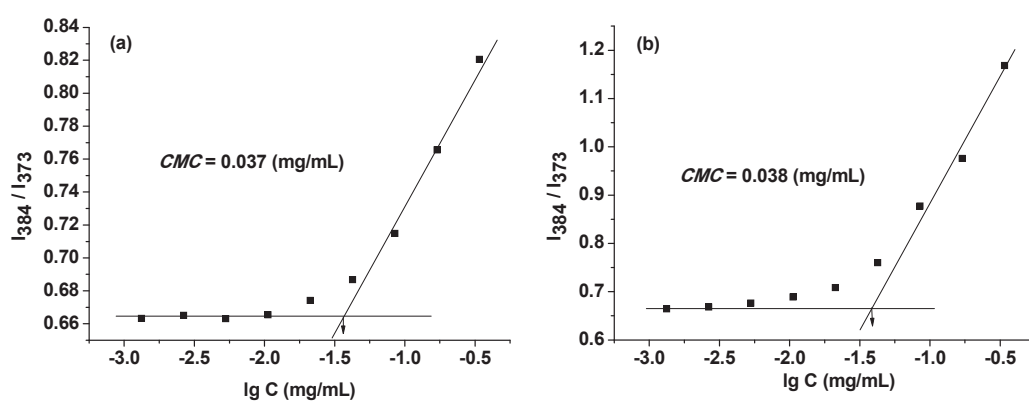


Fig. 8. Plots of  $I_{384}/I_{373}$  versus logarithm of concentration of *l*-PNVCL-*N*<sub>3</sub> (a) and *c*-PNVCL (b).

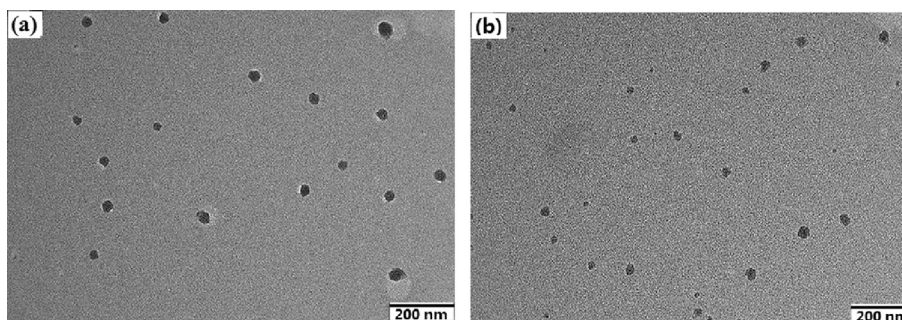


Fig. 9. TEM images of the formed micelles by *l*-PNVCL-*N*<sub>3</sub> (a) and *c*-PNVCL (b).

different concentrations. It can be seen that *c*-PNVCL shows lower LCST values as compared to that of *l*-PNVCL-*N*<sub>3</sub> at all concentrations tested, demonstrating the thermal phase transition is affected by the topology of the polymer. From Fig. 5, we can observe that LCST values of *l*-PNVCL-*N*<sub>3</sub> and *c*-PNVCL have strong concentration dependence. As the polymer concentrations increase from 0.1 to 1.5 mg/mL, LCST values decrease from 36 to 32 °C for *l*-PNVCL-*N*<sub>3</sub>, and from 34 to 29 °C for *c*-PNVCL. Compared with *l*-PNVCL-*N*<sub>3</sub>, *c*-PNVCL shows lower LCSTs at all concentrations tested. These results are similar to the thermal phase transition behavior of linear-PNIPAM-*N*<sub>3</sub> and cyclic-PNIPAM, which are accounted for by the suppression of the hydrogen bond interaction between the cyclic polymers and water molecules due to their topological constraints in comparison with the flexible linear counterpart having free chain ends [17]. It has been reported that

cyclic-PNIPAM possessed broader thermal phase transition range as compared to linear-PNIPAM-*N*<sub>3</sub> [17,18]. In contrast to the case of PNIPAM, *c*-PNVCL solutions undergo a relatively sharp decrease in transmittance, whereas solutions of *l*-PNVCL-*N*<sub>3</sub> exhibit a more gradual decrease in transmittance. The difference could be attributed to the fact that PNVCL and PNIPAM differ in the mechanisms and thermodynamics of the phase transition [37]. PNIPAM exhibits an almost complete independence of LCST on the polymer chain length which is a thermo-responsive phase behavior in water Type II, while the LCST value of PNVCL varies with the polymer chain length and concentration, which shows a “classical” Flory–Huggins thermo-responsive behavior in water (Type I) [47,48]. The effect of cyclic architecture on the thermal phase transition behavior of PNVCL may be different from that of PNIPAM.

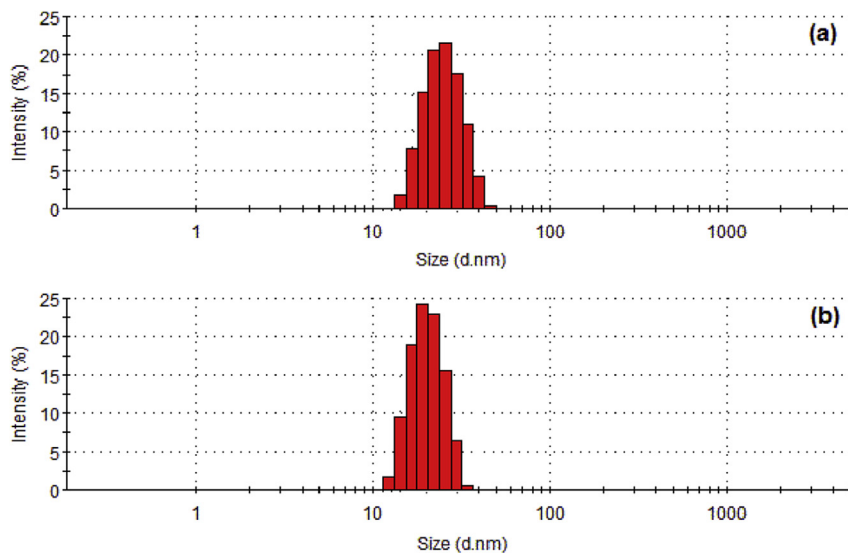


Fig. 10. Size distributions of the formed micelles by *l*-PNVCL- $N_3$  (a) and *c*-PNVCL (b).

DLS was further employed to study the thermoresponsive phase transition behavior of *l*-PNVCL- $N_3$  and *c*-PNVCL in aqueous solution at a concentration of 1.0 mg/mL. The hydrodynamic diameter ( $D_h$ ) of the *l*-PNVCL- $N_3$  and *c*-PNVCL are apparently influenced by the temperature (Fig. 6). The aqueous solution of *l*-PNVCL- $N_3$  and *c*-PNVCL gave a low  $D_h$  around 42 and 28 nm, respectively, when the temperature was below LCST. As temperature was raised progressively, the polymers started to aggregate at their respective LCST and formed micron-size assemblies. Moreover, the aggregation process was completely reversible. These are consistent with the results of turbidimetry measurement.

#### 3.4. Micelle characterization of *l*-PNVCL- $N_3$ and *c*-PNVCL

The presence of hydrophilic cyclic amide groups and hydrophobic carbon–carbon backbone chain means that PNVCL can form a micellar structure when exposed to a selective solvent. Recently, Singh et al. [40] reported that low molecular weight PNVCL was capable of self-assembling to form core–shell (corona) structure micelles in aqueous media. In this study, the formation of micelles from *l*-PNVCL- $N_3$  and *c*-PNVCL were verified by fluorescence technique using pyrene as a probe, TEM and DLS measurements. Fig. 7 shows the fluorescence intensity ratio ( $I_{384}/I_{373}$ ) of pyrene emission spectra as a function of the concentration of *l*-PNVCL- $N_3$  and *c*-PNVCL aqueous solution. It is observed that the change in intensity ratios is negligible below a certain concentration and then increase sharply above that concentration, indicating the formation of micelles. The critical micelle concentration (CMC) was determined from the intersection of two straight lines at the low concentration range. The CMC values of *l*-PNVCL- $N_3$  and *c*-PNVCL were determined to be 0.037 and 0.038 mg/mL (Fig. 8), respectively, indicating the CMC is not influenced significantly by the topology of the polymer. This is coincident with the behavior of some amphiphilic cyclic copolymers and their counterparts [49].

The size and morphology of the micelles were directly observed by TEM as shown in Fig. 9. Both *l*-PNVCL- $N_3$  and *c*-PNVCL self-assembled into spherical micelles, however, there was significant difference in the size. The size of micelles formed by *c*-PNVCL is smaller than that of *l*-PNVCL- $N_3$  (25 nm vs 39 nm, respectively). This is consistent with the studies of self-assembly behavior of amphiphilic cyclic copolymers in aqueous solution [5,50] that

suggests that the more compact self-assembled units results from the lack of chain ends in the cyclic system [51]. The formation of micelles is also supported by DLS measurement. Fig. 10 showed the size distribution of the formed micelles (42 nm for *l*-PNVCL- $N_3$ , 28 nm for *c*-PNVCL), these results were in agreement with that of the TEM.

#### 4. Conclusions

In conclusion, we have demonstrated that well-defined cyclic PNVCL can be successfully synthesized from  $\alpha$ -alkyne- $\omega$ -azide linear precursor at a relatively high concentration (10 mg/mL) via a combination of supramolecular self-assembly and “selective” click cyclization. This high-efficiency synthetic method can be used to synthesize not only thermoresponsive cyclic diblock copolymers but also thermoresponsive cyclic homopolymers and is expected to be generalized to preparation of cyclic NVCL-based copolymers. The solution properties of cyclic PNVCL with its precursor were investigated and compared, and the results revealed that cyclic PNVCL and its linear counterpart can self-assemble to form nanospherical micelles in water. Compared to its linear counterpart, cyclic PNVCL forms smaller aggregates and shows lower LCST and narrower thermal phase transition range.

#### Acknowledgments

The authors gratefully acknowledge support for this work of the National Natural Science Foundation of China (20864003 and 21264017).

#### References

- [1] Jia ZF, Monteiro JM. *J. Polym. Sci. Part A Polym. Chem.* 2012;50:2085–97.
- [2] Yamamoto T, Tezuka Y. *Polym. Chem.* 2011;2:1930–41.
- [3] Ye J, Xu J, Hu JM, Wang XF, Zhang GZ, Liu SY, Wu C. *Macromolecules* 2008;41:4416–22.
- [4] Laurent BA, Grayson SM. *Polym. Chem.* 2012;3:1846–55.
- [5] Zhang BY, Zhang H, Li YJ, Hoskins JN, Grayson SM. *ACS Macro Lett.* 2013;2:845–8.
- [6] Ren MJ, Satoh K, Goh TK, Blencowe A, Nagai K, Ishitake K, Christofferson AJ, Yipanis G, Yarovsky I, Kamigaito M, Qiao GG. *Angew. Chem. Int. Ed.* 2014;53:459–64.
- [7] Michieletto D, Marenduzzo D, Orlandini E, Alexander GP, Turner MS. *ACS Macro Lett.* 2014;3:255–9.

- [8] Córdova ME, Lorenzo AT, Müller AJ, Hoskins JN, Grayson SM. *Macromolecules* 2011;44:1742–6.
- [9] Laurent BA, Grayson SM. *Chem. Soc. Rev.* 2009;38:2202–13.
- [10] Jeong W, Hedrick JL, Waymouth RM. *J. Am. Chem. Soc.* 2007;129:8414–5.
- [11] Laurent BA, Grayson SM. *J. Am. Chem. Soc.* 2006;128:4238–9.
- [12] Zhang YN, Wang GW, Huang JL. *Macromolecules* 2010;43:10343–7.
- [13] Lu DR, Jia ZF, Monteiro JM. *Polym. Chem.* 2013;4:2080–9.
- [14] Tang QQ, Wu Y, Sun P, Chen YM, Zhang K. *Macromolecules* 2014;47:3775–81.
- [15] Stamenović MM, Espeel P, Baba E, Yamamoto T, Tezukab Y, Du Prez FE. *Polym. Chem.* 2013;4:184–93.
- [16] Liu B, Wang H, Zhang L, Yang G, Liu X, Kim I. *Polym. Chem.* 2013;4:2428–31.
- [17] Xu J, Ye J, Liu S. *Macromolecules* 2007;40:9103–10.
- [18] Qiu XP, Tanaka F, Winnik FM. *Macromolecules* 2007;40:7069–71.
- [19] Hoskins JN, Grayson SM. *Macromolecules* 2009;42:6406–13.
- [20] Chen F, Liu G, Zhang G. *J. Polym. Sci. Part A Polym. Chem.* 2012;50:831–5.
- [21] Zhu X, Zhou N, Zhu J, Zhang Z, Zhang W, Cheng Z, Tu Y, Zhu X. *Macromol. Rapid Commun.* 2013;34:1014–9.
- [22] Eugene DM, Grayson SM. *Macromolecules* 2008;41:5082–4.
- [23] Dong YQ, Tong YY, Dong BT, Du FS, Li ZC. *Macromolecules* 2009;42:2940–8.
- [24] Wan X, Liu T, Liu S. *Biomacromolecules* 2011;12:1146–54.
- [25] Fan X, Huang B, Wang G, Huang J. *Macromolecules* 2012;45:3779–86.
- [26] Ge ZS, Zhou YM, Xu J, Liu HW, Chen DY, Liu SY. *J. Am. Chem. Soc.* 2009;131:1628–9.
- [27] Lonsdale DE, Bell CA, Monteiro MJ. *Macromolecules* 2010;43:3331–9.
- [28] Roy D, Brooks WLA, Sumerlin BS. *Chem. Soc. Rev.* 2013;42:7214–43.
- [29] Li Y, Pan S, Zhang W, Du Z. *Nanotechnology* 2009;20:06510.
- [30] Junk MJN, Li W, Schlüter AD, Wegner G, Spiess HW, Zhang AF, Hinderberger D. *J. Am. Chem. Soc.* 2011;133:10832–8.
- [31] Nagase K, Yuk SF, Kobayashi J, Kikuchi A, Akiyama Y, Kanazawa H, Okano T. *J. Mater. Chem.* 2011;21:2590–3.
- [32] Liu J, Detrembleur C, Hurtgen M, Debuigne A, De Pauw-Gillet MC, Mornet S, Etienne D, Jérôme C. *Polym. Chem.* 2014;5:5289–99.
- [33] Bi YM, Yan CX, Shao LD, Wang YF, Ma YC, Tang G. *J. Polym. Sci. Part A Polym. Chem.* 2013;51:3240–50.
- [34] Prabaharan M, Grailer JJ, Steeber DA, Gong SQ. *Macromol. Biosci.* 2009;9:744–53.
- [35] Rejinold NS, Chennazhi KP, Nair SV, Tamura H, Jayakumar R. *Carbohydr. Polym.* 2011;83:776–86.
- [36] Beija M, Marty JD, Destarac M. *Chem. Commun.* 2011;47:2826–8.
- [37] Ramos J, Imazb A, Forcada J. *Polym. Chem.* 2012;3:852–6.
- [38] Hay RW, Lawrance GA. *J. Chem. Soc. Perkin Trans.* 1975;1(6):591–3.
- [39] Yang Y, Li J, Hu M, Chen L, Bi Y. *J. Polym. Res.* 2014;21:549.
- [40] Singh P, Srivastava A, Kumar R. *J. Polym. Sci. Part A Polym. Chem.* 2012;50:1503–14.
- [41] Jiang X, Li Y, Lu G, Huang X. *Polym. Chem.* 2013;4:1402–11.
- [42] Lu XJ, Gong SL, Meng LZ, Li C, Yang S, Zhang LF. *Polymer* 2007;48:2835–42.
- [43] Xia Y, Yin X, Burke NAD, Stöver HDH. *Macromolecules* 2005;38:5937–43.
- [44] Oike H, Imaizumi H, Mouri T, Yoshioka Y, Uchibori A, Tezuka Y. *J. Am. Chem. Soc.* 2000;122:9592–9.
- [45] Schappacher M, Deffieux A. *Macromolecules* 2001;34:5827–32.
- [46] Hogen-Esch TE. *J. Polym. Sci. Part A Polym. Chem.* 2006;44:2139–55.
- [47] Meeussen F, Nies E, Berghmans H, Verbrugghe S, Goethals E, Du Prez F. *Polymer* 2000;41:8597–602.
- [48] Maeda Y, Nakamura T, Ikeda I. *Macromolecules* 2002;35:217–22.
- [49] Honda S, Yamamoto T, Tezuka Y. *J. Am. Chem. Soc.* 2010;132:10251–3.
- [50] Minatti E, Viville P, Borsali R, Schappacher M, Deffieux A, Lazzaroni R. *Macromolecules* 2003;36:4125–33.
- [51] Poelma JE, Ono K, Miyajima D, Aida T, Satoh K, Hawker CJ. *ACS Nano* 2012;6:10845–54.